Boyer, H., Bzdek, B., Reid, J., & Dutcher, C. (2017). A Statistical Thermodynamic Model for Surface Tension of Organic and Inorganic Aqueous Mixtures. *Journal of Physical Chemistry A*, *121*(1), 198-205. https://doi.org/10.1021/acs.jpca.6b10057

A Statistical Thermodynamic Model for Surface Tension of Organic and Inorganic Aqueous Mixtures

*Hallie C. Boyer[a], Bryan R. Bzdek[b], Jonathan P. Reid[b] and Cari S. Dutcher[a]**

(cdutcher@umn.edu)

[a]Department of Mechanical Engineering, University of Minnesota, Twin Cities, Minneapolis, MN 55455, USA. [b]School of Chemistry, University of Bristol, BS8 1TS, UK.

Abstract

The surface composition and tensions of aqueous aerosols govern a set of processes that largely determine the fate of particles in the atmosphere. Predictive modeling of surface tension can provide significant contributions to studies of atmospheric aerosol effects on climate and human health. A previously derived surface tension model (Wexler and Dutcher, *J. Phys. Chem. Lett.*, 2013; Boyer et al. *J. Phys. Chem. Lett.*, 2015) for single solute aqueous solutions used adsorption isotherms and statistical mechanics to enable surface tension predictions across the entire concentration range as a function of solute activity. Here, we extend the model derivation to address multicomponent solutions and demonstrate its accuracy with systems containing mixtures of electrolytes and organic solutes. Binary model parameters are applied to the multicomponent model, requiring no further parametrization for mixtures. Five ternary systems are studied here and represent three types of solute combinations: organic-organic (glycerol-ethanol), electrolyte-organic (NaCl-succinic acid, NaCl-glutaric acid), and electrolyte-electrolyte (NaCl-KCl and NH_4NO_3-$(NH_4)_2SO_4$). For the NaCl-glutaric acid system, experimental measurements of picoliter droplet surface tension using aerosol optical tweezers show excellent agreement with the model predictions.

Introduction

The surface tension of atmospheric aqueous aerosol particles is an essential factor in determining growth processes, heterogeneous chemistry, phase transitions, equilibrium morphology, and cloud activation.[1,2] Chemical constituents known to be present in atmospheric aerosol are both organic (e.g. organic acids) and inorganic (e.g. ammonium salts). Most organic solutes lower the surface tension of pure water[3] by adsorbing at the surface. Inorganic electrolytes tend to remain in the solution interior to due attractive ion-water interactions, which results in a relative destabilizing of water interactions at the surface over in the bulk and an increase in surface tension with respect to pure water. In solutions containing mixtures, the effect of individual species on surfaces is convoluted.

There are recent experimental and computational efforts to understand surface propensities of solutes in complex aqueous solutions. Öhrwall and coworkers[4] use synchrotron radiation spectroscopy to show that the addition of ammonium electrolytes enhances surface density of carboxylate ions in aqueous organic acid solutions. They propose that instead of a salting-out effect brought on by the salt, a surface bilayer of ammonium ions enhances deprotonation of the neutral species on the surface. Through molecular simulations of Venkateshwaran et al.[5], it was shown that ions at the surface of aqueous solutions exhibit unexpected behavior such as attraction between like charges in small ions when they are close to the vapor phase.

In the atmosphere, surface composition affects other surface-based properties and processes of aqueous aerosol. One effect of organic molecules residing on surfaces is that they can lower the critical supersaturation,[6] facilitating cloud droplet activation.[7] Organics can also enhance reaction rates between the liquid surface and ambient vapor, specifically with gaseous molecular chloride and bromide.[8] Recently, Reuhl et al.[1] and Noziere[9] highlighted the importance of

accounting for surface tension depression by organic solutes on aqueous surfaces in predictions of cloud activation. In aqueous solutions of citric acid and sodium bromide, surface composition and resulting effects on uptake kinetics have been quantified using X-ray photoelectron spectroscopy (XPS).[10] Ammonium sulfate tends to depress the equilibrium vapor pressure of aqueous dicarboxylic acids, thus inhibiting partitioning into the gas phase.[11] Frosch et al.[12] have studied cloud activation as affected by solution properties (water activity) and surface properties (surface tension) in aqueous phases containing organic acids and inorganic electrolytes. The effects of solute mixtures on aqueous surfaces must be better understood to accurately predict the fate of aerosol particles in the atmosphere.

There are a few existing surface tension models where the binary versions are successfully extended to mixtures (a solvent plus two or more solutes) with no additional parameters[13–18] that are constructed to treat each class of solute separately. Li et al.[13] developed a surface tension model using an adsorption isotherm similar to Langmuir that reaches solubility limits of many aqueous electrolytes with both single and multiple solutes as a function of osmotic coefficient. Extending the model to mixtures required no further parameterization. Solute activity was used to represent concentration, for which they used Pitzer's equation[19]. Li and Lu[14] also developed a multicomponent surface tension model, but instead covered only liquid organics solutes instead of electrolyte mixtures. They performed molecular simulations assuming Lennard-Jones liquids with the convenience of using surface tensions of pure liquids to determine parameters. Hu and Lee[15] demonstrate a simple thermodynamic model where surface tension is a function of water activities of the mixture and binary solutions of each solute at the same ionic strength. Finally, Lee and Hildeman[16,17] measured surface tension for aqueous solutions containing mixtures of dicarboxylic acids and fitted their results using the Szyzkowski equation[20] by extending the equation to ternary

solutions. To our knowledge, there are currently no available models that sufficiently handle electrolyte and organic mixtures in the same solution without further parameterization and that can accurately extend to supersaturated concentrations. We present here a statistical thermodynamic model of surface tension for ternary systems using only optimized parameters from the binary cases[21–23] that is valid across the entire concentration range and accommodates organic and inorganic solutes in the same system.

In our prior work, a theoretical framework was developed in *solution* using adsorption isotherms, "hydrating" solutes with multi-layers with short-range energy parameters associated with each layer and long-range Coulombic interactions for charged solutes.[24–28] Using statistical mechanics, the model gave predictions of multicomponent solution properties, such as water activity, osmotic coefficient, and solute activity, as a function of solute molality. Next, the adsorption isotherm was applied to the *surface* of a single solute aqueous solution,[21] with the important distinction of solutes being the adsorbates, partitioning to the surface phase by displacing water molecules. Again using statistical mechanics, partition functions were written for the two regions: at the surface, representing the possible configurations of solvent and solute molecules that partition to the interface; and in the bulk, representing solute mixing between the surface and the bulk. While several multi-layers were necessary to predict water activity, the surface tension model was successful in using the surface as the monolayer, and the bulk as a single multi-layer. Using the same theoretical framework as the binary case, the statistical mechanical derivation for a multicomponent surface tension model and several applications are shown in the next section.

Excellent model agreement is shown with measurements from various sources. In particular, a novel approach to directly measure the surface tension of airborne picoliter droplets

is used to compare to model results in the supersaturation regime.[29] This approach relies on the measurement of damped shape oscillations resulting from the coalescence of two airborne droplets. Building off of the parameterizations of the binary model,[21-23] predictions for ternary systems are demonstrated with absolutely no fitting. Model derivations for an arbitrary number of solutes are shown in the supporting information so the model can be further extended as needed.

Statistical Mechanical Derivation

Consider two solute species A and B in aqueous solution. The maximum number of waters at the surface is N_{WS}; each solute molecule displaces r_A and r_B waters from the surface.

The partition function for the surface for solute A is

$$\Omega_{surface,A} = \frac{N_{WS}!_{(r_A)}}{(N_{WS} - r_A N_{AS})!_{(r_A)}\,(r_A N_{AS})!_{(r_A)}} \quad (1)$$

and for solute B, the number of configurations remaining on the leftover adsorption sites is

$$\Omega_{surface,B} = \frac{(N_{WS} - r_A N_{AS})!_{(r_B)}}{(N_{WS} - r_A N_{AS} - r_B N_{BS})!_{(r_B)}\,(r_B N_{BS})!_{(r_B)}} \quad (2)$$

where N_{AS} and N_{BS} are the numbers of molecules A and B displacing waters on the surface. In the single solute case,[21] r is a model parameter that represents the average number of water molecules displaced from the surface by a solute molecule and therefore is an indicator of size and surface density. In recent work,[23] $\bar{r}$ was used to represent a collective effect of two solutes in the development of a multicomponent model that did not distinguish between solute sizes. Here, r_A and r_B are used to treat individual size effects of each species. Multiplying eqs 1 and 2 together, the surface partition function is

$$\Omega_{surface,AB} = \frac{N_{WS}!_{(r_A)}\,(N_{WS} - r_A N_{AS})!_{(r_B)}}{(N_{WS} - r_A N_{AS})!_{(r_A)}\,(r_A N_{AS})!_{(r_A)}\,(N_{WS} - r_A N_{AS} - r_B N_{BS})!_{(r_B)}\,(r_B N_{BS})!_{(r_B)}} \quad (3)$$

resulting in a partition function that gives solute A an arbitrary preference for surface adsorption sites over B. $\Omega_{surface,AB}$ must not change if alternatively written with solute B in eq 1 and solute A in eq 2:

$$\Omega_{surface,BA} = \frac{N_{WS}!_{(r_B)}\,(N_{WS} - r_B N_{BS})!_{(r_A)}}{(N_{WS} - r_B N_{BS})!_{(r_B)}\,(r_B N_{BS})!_{(r_B)}\,(N_{WS} - r_A N_{AS} - r_B N_{BS})!_{(r_A)}\,(r_A N_{AS})!_{(r_A)}} \quad (4)$$

Therefore, to establish symmetry and therefore preserve equal probabilities of A and B surface adsorption, the surface partition function is written as

$$\Omega_{surface} = \left(\Omega_{surface,AB}\Omega_{surface,BA}\right)^{1/2} \quad (5)$$

Next, the bulk partition functions represent mixing between surface and bulk phases. N_{AB} is the number of A molecules in the bulk and $N_A = N_{AB} + N_{AS}$, so the bulk partition function for A is

$$\Omega_{bulk,A} = \frac{N_A!}{N_{AS}!\,N_{AB}!} = \frac{N_A!}{N_{AS}!\,(N_A - N_{AS})!} \quad (6)$$

and for B,

$$\Omega_{bulk,B} = \frac{N_B!}{N_{BS}!\,N_{BB}!} = \frac{N_B!}{N_{BS}!\,(N_B - N_{BS})!} \quad (7)$$

where $N_B = N_{BB} + N_{BS}$ and N_{BB} is the number of B molecules in the bulk. Letting $\chi = N_{WS} - r_A N_{AS} - r_B N_{BS}$, the full partition function is

$$\Omega = \Omega_{surface}\Omega_{bulk} = \Omega_{surface}\Omega_{bulk,A}\Omega_{bulk,B} = \frac{N_A!\,N_B!}{(r_A N_{AS})!_{(r_A)}\,(r_B N_{BS})!_{(r_B)}\,N_{AS}!\,(N_A - N_{AS})!\,N_{BS}!\,(N_B - N_{BS})!} \times \left(\frac{N_{WS}!_{(r_A)}\,(N_{WS} - r_A N_{AS})!_{(r_B)}\,N_{WS}!_{(r_B)}\,(N_{WS} - r_B N_{BS})!_{(r_A)}}{\chi!_{(r_A)}\,\chi!_{(r_B)}\,(N_{WS} - r_A N_{AS})!_{(r_A)}\,(N_{WS} - r_B N_{BS})!_{(r_B)}}\right)^{1/2} \quad (8)$$

Configurational entropy is obtained from Boltzmann's formula, $S = k\ ln(\Omega_{surface}\Omega_{bulk})$. Using Stirling's approximation including skips $ln(N!_r) = \frac{N}{r} ln\frac{N}{r} - \frac{N}{r}$,

$$ln\Omega = N_A ln\frac{N_A}{(N_A - N_{AS})} + N_B ln\frac{N_B}{(N_B - N_{BS})} + \frac{N_{WS}}{2r_A} ln\frac{N_{WS}(N_{WS} - r_B N_{BS})}{\chi(N_{WS} - r_A N_{AS})}$$
$$+ \frac{N_{WS}}{2r_B} ln\frac{N_{WS}(N_{WS} - r_A N_{AS})}{\chi(N_{WS} - r_B N_{BS})} + \frac{r_A N_{AS}}{2r_B} ln\frac{\chi}{(N_{WS} - r_A N_{AS})} \quad (9)$$
$$+ \frac{r_B N_{BS}}{2r_A} ln\frac{\chi}{(N_{WS} - r_B N_{BS})} + \frac{N_{AS}}{2} ln\frac{\chi(N_{WS} - r_A N_{AS})(N_A - N_{AS})^2}{{r_A}^2 {N_{AS}}^4}$$
$$+ \frac{N_{BS}}{2} ln\frac{\chi(N_{WS} - r_B N_{BS})(N_B - N_{BS})^2}{{r_B}^2 {N_{BS}}^2}$$

The system energy is the sum of all molecular energies, represented by energies of waters on the surface (ε_{WS}) and in the bulk (ε_{WB}) and solute molecules on the surface and bulk (ε_{AS}, ε_{AB}, ε_{BS}, ε_{BB}).

$$E = -N_{WS}\varepsilon_{WS} - N_{WB}\varepsilon_{WB} - N_{AS}\varepsilon_{AS} - N_{AB}\varepsilon_{AB} - N_{BS}\varepsilon_{BS} - N_{BB}\varepsilon_{BB} \quad (10)$$

which can be rearranged as

$$E = -N_{WS}\Delta\varepsilon_{WS} - N_W\varepsilon_{WB} - N_{AS}\Delta\varepsilon_{AS} - N_A\varepsilon_{AB} - N_{BS}\Delta\varepsilon_{BS} - N_B\varepsilon_{BB} \quad (11)$$

where the total number of waters in the system is $N_W = N_{WS} + N_{WB}$. Assuming system energy is approximately the enthalpy due to negligible pressure and volume changes and combining eqs 9 and 11, Gibbs free energy is

$$G/kT \approx E/kT - ln\Omega \quad (12)$$

where S_w is the occupied area of one water molecule (0.1 nm^2). Taking the derivative of eq 12 with respect to area and letting σ represent solution surface tension and σ_w the surface tension of pure water (71.98 mN/m at 298 K) found in the limit of zero solute, then

$$\sigma = \sigma_W + \frac{kT}{2r_A S_w} ln\left[\frac{\chi(N_{WS} - r_A N_{AS})}{N_{WS}(N_{WS} - r_B N_{BS})}\right] + \frac{kT}{2r_B S_w} ln\left[\frac{\chi(N_{WS} - r_B N_{BS})}{N_{WS}(N_{WS} - r_A N_{AS})}\right] \quad (13)$$

Expressions for the activities of solute A (a_A) and solute B (a_B) are obtained from taking the derivative of eq 8 with respect to N_A and N_B, respectively, resulting in

$$K_A a_A = 1 - \frac{N_{AS}}{N_A} \quad (14)$$

$$K_B a_B = 1 - \frac{N_{BS}}{N_B} \quad (15)$$

where $K_A = exp\left(\frac{\varepsilon_{AB}}{kT}\right)$ and $K_B = exp\left(\frac{\varepsilon_{BB}}{kT}\right)$. The condition of equilibrium partitioning between the surface phase and bulk phase is imposed by minimizing eq 12 with respect to N_{AS} and N_{BS}, resulting in

$$C_A = exp\left(\frac{\Delta\varepsilon_{AS}}{kT}\right) = \left(\left(\frac{\left(\frac{(N_{WS} - r_A N_{AS})}{\chi}\right)^{r_A/r_B}}{\chi(N_{WS} - r_A N_{AS})}\right)^{1/2} \frac{r_A {N_{AS}}^2}{N_A - N_{AS}}\right) \quad (16)$$

$$C_B = exp\left(\frac{\Delta\varepsilon_{BS}}{kT}\right) = \left(\left(\frac{\left(\frac{(N_{WS} - r_B N_{BS})}{\chi}\right)^{r_B/r_A}}{\chi(N_{WS} - r_B N_{BS})}\right)^{1/2} \frac{r_B {N_{BS}}^2}{N_B - N_{BS}}\right) \quad (17)$$

In the case of a single solute A ($N_{BS} = 0$), eqs 14 and 16 are be rearranged and substituted into eq 13, which results in

$$\sigma = \sigma_w + \frac{kT}{r_A S_w} Ln\left(\frac{1 - K_A a_A}{1 - K_A a_A (1 - C_A)}\right) \quad (18)$$

which is the same form as the binary model from prior work by Wexler and Dutcher.[21] In the case of two solutes, if r_A and r_B are not treated separately, but instead as a unified quantity $\bar{r}$, eqs 14-17 could be combined to give

$$\sigma = \sigma_w - \frac{kT}{\bar{r} S_w} Ln\left(1 + \frac{C_A K_A a_A}{(1 - K_A a_A)} + \frac{C_B K_B a_B}{(1 - K_B a_B)}\right) \quad (19)$$

as shown by Boyer and Dutcher.[23] However, the multicomponent model for solutes of varied size, derived in this work, does not have a single analytic solution for surface tension of solution as a function of concentrations. The model is rather a system of nonlinear equations (eqs 13-17) that require numerical methods to solve, as detailed in the next section, to get predictions of surface tension, σ, as a function of activities a_A and a_B.

Numerical Methods

The set of equations 13-17 consist of model parameters (r_A, K_A, C_A, r_B, K_B, and C_A), quantities representing waters and solutes at the surface (N_{WS}, N_{AS}, N_{BS}, N_A, and N_B), solute activities (a_A and a_B) and solution surface tension (σ). In recent work by Boyer et al.,[22] parameters $r, K,$ and C for several electrolyte and organic binary aqueous solutions were determined with the surface tension model from Wexler and Dutcher.[21] In the current work, those parameters identified for electrolytes and glycerol are applied as constants in the new model for ternary solutions. For organic solutes ethanol, glutaric acid, and succinic acid, new parameters were determined from the binary model shown in eq 18, since in prior work[22,23] a modified form of the model was used for surface active species with a reduced number of parameters. All parameter values and data sources used in this work can be found in Table 1.

For concentrations, activities for each solute a_A and a_B are calculated from the modeling work of Ohm et al.,[27] a thermodynamic model of solution properties using methods of statistical mechanics of multilayer adsorption similar to those used to derive the current model at the interface. The remaining unknowns are the N quantities N_{WS}, N_{AS}, N_{BS}, N_A and N_B and surface tension σ. Since N_{WS} defines how many waters exist at the interface without solute adsorption, it is set at an arbitrary value. This leads to five unknowns are N_{AS}, N_{BS}, N_A, N_B and σ. Note that if there are zero solutes, the resulting value of σ will be σ_w no matter what value N_{WS} is used.

Equations 13-17 are a system of five nonlinear equations with five unknowns (N_{AS}, N_{BS}, N_A, N_B and σ). To simplify the system to two equations, eqs 14 and 15 are substituted into 16 and 17, respectively, resulting in

$$C_A = \left(\left(\frac{\left(\frac{(N_{WS} - r_A N_{AS})}{\chi} \right)^{r_A/r_B}}{\chi (N_{WS} - r_A N_{AS})} \right)^{1/2} \frac{r_A N_{AS}(1 - K_A a_A)}{K_A a_A} \right) \quad (20)$$

$$C_B = \left(\left(\frac{\left(\frac{(N_{WS} - r_B N_{BS})}{\chi} \right)^{r_B/r_A}}{\chi (N_{WS} - r_B N_{BS})} \right)^{1/2} \frac{r_B N_{BS}(1 - K_B a_B)}{K_B a_B} \right) \quad (21)$$

Here, there are two equations (20 and 21) and two unknowns (N_{AS} and N_{BS}). Surface tension is found by substituting the solutions from eqns 14-17 into eq 13, again noting that there are no ternary mixing parameters in the model.

Experimental Methods

For the binary NaCl-water and glutaric acid-water systems as well as for the ternary NaCl-glutaric acid-water system, model estimations were compared to surface tension measurements performed directly on 5-10 μm radius aerosol droplets using holographic aerosol optical tweezers.[27] Because the measurement is made on aerosol rather than bulk solutions, measurements on supersaturated solute states are accessible by this approach. The experimental apparatus has been described in detail previously.[29–32] In a typical experiment, two aqueous droplets were captured in two separate optical traps by nebulizing (Omron NE U22) a solution into a humidity-controlled trapping chamber. The two optical traps were created using a spatial light modulator (LCOS-SLM, Hamamatsu X10468) that dynamically shapes the phase front of a continuous wave 532 nm laser (Laser Quantum, Opus 3QW). The relative positions of these traps are controlled by

a pre-calculated sequence of kinoforms, and the rate at which the kinoforms were changed was user-controlled. Once the trap separation was sufficiently small, the two droplets coalesced to one composite droplet. The capture and relative position of the droplets was monitored with a camera (Dalsa Genie HM 640, CMOS) utilizing widefield illumination with a high power LED (Thorlabs, 470 nm). Inelastic backscattered (Raman) laser light was directed to a 0.5 m focal length spectrograph (Princeton Instruments, Action Spectra Prop SP-2500). The Raman spectrum from a spherical droplet consists of a broad underlying Stokes band with superimposed resonant structure at wavelengths commensurate with whispering gallery modes (WGMs; see Fig. 1a), from which the radius, refractive index, and dispersion can be determined with accuracies better than 2 nm, 0.0005, and 3×10^{-8} cm respectively.[33] Elastic backscattered laser light (see Fig. 1b) was collected using a silicon photodetector (Thorlabs, DET 110) and recorded using a low-load, 12 bit ADC resolution, 2.5 GS·s^{-1} sample rate oscilloscope (LeCroy, HDO 6034-MS).

The basic measurement involves monitoring the damped oscillations in droplet shape that occur upon the coalescence of two low viscosity droplets. The time dependence of the changing shape of the composite droplet in the microseconds following coalescence is determined from highly time-resolved (~100 ns time resolution) measurements of the varying intensity of the elastic backscattered light, which corresponds to changes in droplet shape.[34] The frequency of these shape oscillations gives the surface tension of the composite droplet through eq 22[35,36]

$$\sigma = \frac{a^3 \rho \omega_l^2}{l(l-1)(l+2)} \qquad (22)$$

where σ is the composite droplet surface tension, l is the mode order (a characteristic deformation in droplet shape), ω_l is the angular oscillation frequency of a given mode order, a is the droplet radius, and ρ is the droplet density. In general, surface tensions retrieved by this approach have an accuracy and precision better than ±1 mN/m.

Figure 1 shows examples of experimental data for a sodium chloride droplet with high surface tension (σ = 82 mN/m, blue traces) and for a glutaric acid droplet with low surface tension (σ = 57 mN/m, red traces). In Fig. 1a, a representative Raman spectrum is shown for the coalesced droplet in each experiment. The positions of the WGMs are used to extract the droplet radius and refractive index at 650 nm with high precision. From the measured refractive index, several droplet properties (solute concentration, density, and viscosity) are obtained through parametrizations of bulk data.[37] Fig. 1b shows the elastic backscatter intensity during the coalescence event for both droplets. The difference in intensity results from the differing droplet sizes. The intensity maxima and minima correspond to the extremes in droplet shape distortion.[29,34] It is clear from the elastic backscatter intensity that the oscillation frequency is higher for the NaCl droplet, which is a smaller droplet and has a higher surface tension. The Fast Fourier Transform is applied to the elastic backscatter intensity to give Fig. 1c, which shows the droplet oscillation frequency for each droplet, with the frequency for the *l*=2 mode most prominent as this is the mode that persists for the longest time during the shape relaxation. From the droplet oscillation frequency, radius, and refractive index, it is possible to quantify the droplet surface tension through eq 22.

Results

In Figure 2, surface tension measurements are compared to predictions for five different ternary aqueous solutions, demonstrating that the model works equally well for systems containing two electrolytes, two organics, or one organic and one electrolyte. Excellent agreement is found between predictions and measurements for the following systems: NaCl + KCl, NaCl + succininc acid, NaCl + glutaric acid, ethanol + glycerol, and NH_4NO_3 + $(NH_4)_2SO_4$. The rmse of fit, $rmse = \sqrt{\sum_{i=1}^{n_p}(\sigma_i^{data} - \sigma_i^{pred})^2/n_p}$, and data sources are in Table 2.

Next, in Figures 3-5, a specific case for each type of system (electrolyte-organic, organic-organic, electrolyte-electrolyte) is examined to demonstrate that the surface tension is calculated as a function of activity of each solute and that reasonable predictions can be made in the absence of data. For all solutes except organic acids, solute activities in mixtures are found from the solution property modeling work using the adsorption isotherm of Dutcher et al.[24–26] and Ohm et al.[27] For organic acids, activities are found assuming ideal mixing with Raoult's Law, which was shown to work well for these systems when predicting surface tension.[23] Surface tension versus concentration curves in Figures 3-5 are predictions in which the system composition varies from zero solute (pure water) to zero water (pure solute), while the ratio of solutes is held constant as water content changes.

For several solute species (glycerol, ammonium nitrate, ammonium sulfate, potassium chloride), binary model parameters were determined in recent work in which parameters were reduced through correlations with physico-chemical properties, towards fully predictive surface tension modeling of binary solutions (Boyer et al. *J. Phy. Chem. Lett.* 2015). Binary predictions for the other solutes in this study (ethanol, NaCl, glutaric acid, succinic acid) are found by fitting eq 18 to bulk data and optimizing the three model parameters $r, K,$ and C (Table 1). The surface tension of pure solute, σ_s, can also be used as a parameter when eq 18 is evaluated in the limit of pure solute. If σ_s is a known quantity, as is the case for many liquid organics, then it can eliminate a parameter. Binary predictions for both solutes are found by fitting eq 18 to bulk data and optimizing the three model parameters $r, K,$ and C. Model predictions for ternary solutions are found using methods detailed in the Numerical Methods section. As mole ratio increases to favor one solute, the curves progress towards the corresponding binary curve, and correctly limit to the binary case in the limit of one solute.

Electrolyte + organic + water. Model application to ternary aqueous mixtures containing an electrolyte (NaCl) and an organic (glutaric acid) are shown in Figure 3 as well as their respective binary curves. For the first time, we compare binary model predictions to surface tension measurements beyond the solubility limit. Ternary predictions are shown for a mass ratio of 1:1. Supporting data for binary NaCl, binary glutaric acid, and the mixture are provided by experiments using optical tweezers detailed in Experimental Methods. The optical tweezers data are also presented here for binary NaCl and glutaric acid aqueous solutions that extend into the supersaturated regime. As shown by the red and blue lines and full symbols in Figure 3, there is excellent agreement between model predictions and experiments.

For organic and inorganic aqueous mixtures not discussed here, a "salting out" phenomenon may occur in which strongly dissolved salts force organic molecules out of solution, thereby driving them to the surface, and in turn lowering surface tension below that of the organic salt-free solution. The model successfully predicts surface tension of mixtures in Figure 3 by allowing organics and electrolytes to compete for surface adsorption sites with equal probability. To capture salting out effects, a new parameter would be needed to account for solute-solute interactions, either in the surface tension model[21–23] or in the solution activity model.[24–28]

Organic + organic + water. In Figure 4, model prediction curves and data are shown at various constant mole ratios. Mixture data for equimolal solutions, or concentrations with mole ratio 1:1, are in close agreement with predictions. Also, 1:1 surface tensions are much closer to the ethanol curve, suggesting that ethanol has a stronger influence on solution surface tension than glycerol. The additional curves shown in Figure 4 exhibit key capabilities of the model: sensitivity to mole ratio as well as specific effects of each compound. As the mole ratio changes, predictions

tend toward the appropriate binary curve, while it is also clear that ethanol has a dominant effect at the surface.

Electrolyte + electrolyte + water. Model application to aqueous mixtures containing two electrolytes (ammonium nitrate and ammonium sulfate) are shown in Figure 5. Between the binary curves for each solute are model runs for different fixed mole ratios, accompanied by supporting data for the mole ratio 1:1 taken using a Wilhelmy plate (Digital Tensiometer K10ST by Krüss). Both binary fits use a single model parameter, *r*, where others have been eliminated through physical interpretation in recent work.[22] For ammonium sulfate, *rmse* for the single parameter fit was 0.999, and for ammonium nitrate, *rmse* was 0.146. When applied to the model presented here, the higher error for binary ammonium sulfate propagates into mixture predictions. Allowing three model parameters to vary instead of one decreases the error for ammonium sulfate to an *rmse* of 0.219 (plot shown in Supplemental Information).

Summary

Based on a previously derived surface tension model for binary aqueous solutions[21] that uses adsorption isotherms at the interface of solution, we have derived a model that handles two separate solutes and is a function of solute concentration and solute ratio. The adsorption isotherm framework[24–27] was developed beforehand to predict solution properties and subsequently applied to the interface. It was then demonstrated that the surface tension binary model works equally well for organic and electrolyte solutes,[21,22] and can be extended to partially dissociating organic acids by decoupling a single model parameter.[23] Here, we present a multicomponent surface tension model for aqueous solutions containing two solutes and demonstrate its versatility by applying it to mixtures of water soluble organic and inorganic compounds. The efficacy of the model is shown by comparing predictions of ternary solutions to data. Although data for ternary solutions are

scarce, there is remarkable agreement in cases where data are available for comparison with model predictions. Surface tension measurements for systems of aqueous NaCl, glutaric acid, and a mixture of the two are obtained using optical tweezers, which have the capability of measuring surface tension of picolitre droplets in supersaturated states. The overall excellent agreement between model predictions and data from bulk and optical tweezers measurements of ternary systems shows strong potential for adapting the model to solutions of increasing complexity.

solute	**r**	**K**	**C**	σ_s	***rmse***	**Data ref.**
ethanol	2.950	$9.348*10^{-8}$	$3.743*10^{8}$	22.20	1.425	[38]
NaCl	-19.89	0.9900	$3.101*10^{4}$	101.5	0.393	[39]
glutaric acid	9.663	$9.700*10^{-3}$	$4.526*10^{4}$	46.13	0.331	[40]
succinic acid	11.28	0.9579	312.4	39.62	0.128	[40]

Table 1: Parameters from binary modeling that are used in eqs 13-17. In the last column. σ_s represents pure solute surface tension (mN/m) at 298 K. For the alcohols, σ_s is known. For all others, σ_s is a model parameter.

mixture	rmse	data ref./meas.
Ethanol + glycerol	1.379	[41]
$NH_4NO_3 + (NH_4)_2SO_4$	0.424	Wilhelmy plate
NaCl + succinic acid	0.218	[42]
NaCl + glutaric acid	1.013	optical tweezers
NaCl + KCl	0.420	[43]

Table 2: Mixture name, error (rmse) for the model predictions and available data for each system, and data references (ref.) or measurement techniques (meas.).

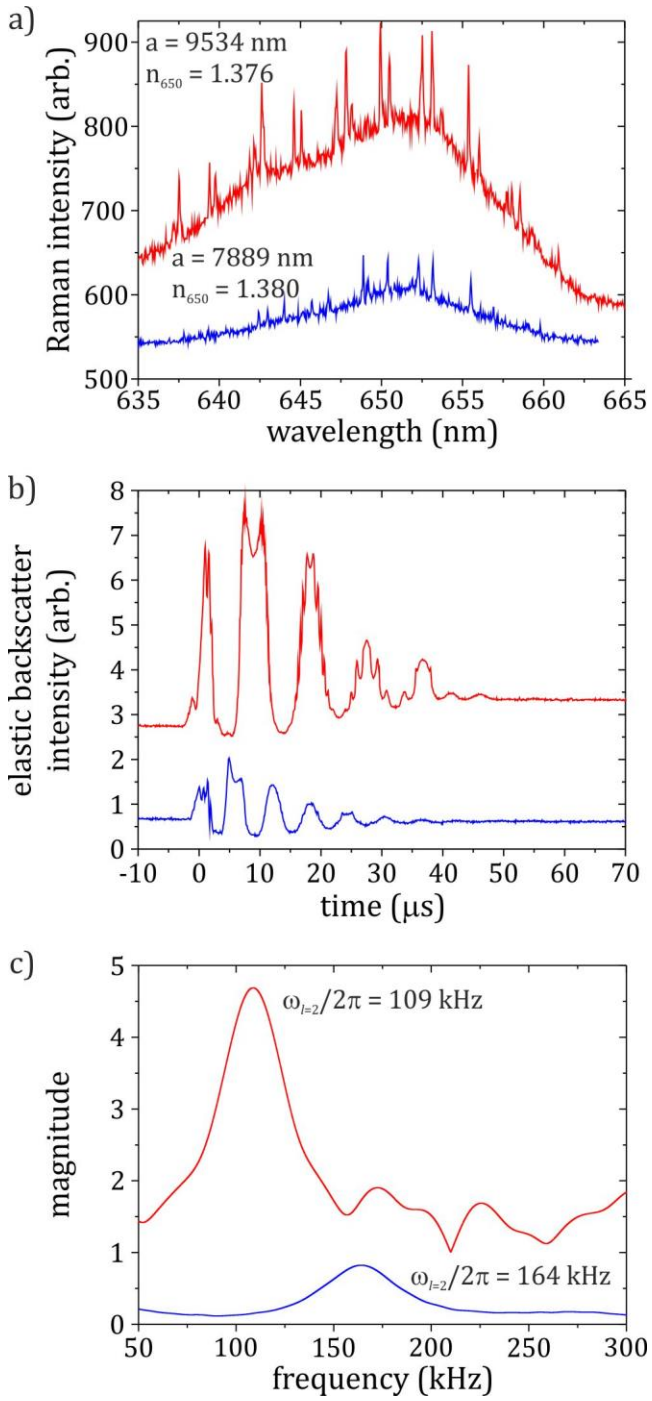

Figure 1: Holographic optical tweezers measurements require simultaneous acquisition of the Raman spectrum of a coalesced droplet and the elastic backscattered light from the coalescence event. Part a) shows representative Raman spectra for a composite sodium chloride droplet (blue trace) and glutaric acid droplet (red trace) immediately after the coalescence event. The best fit

radius and refractive index are given for each droplet. The elastic backscatter intensity for both experiments are shown in part b). Part c) shows the Fast Fourier Transform of part b) to determine the droplet shape oscillation frequency, which is reported in the figure.

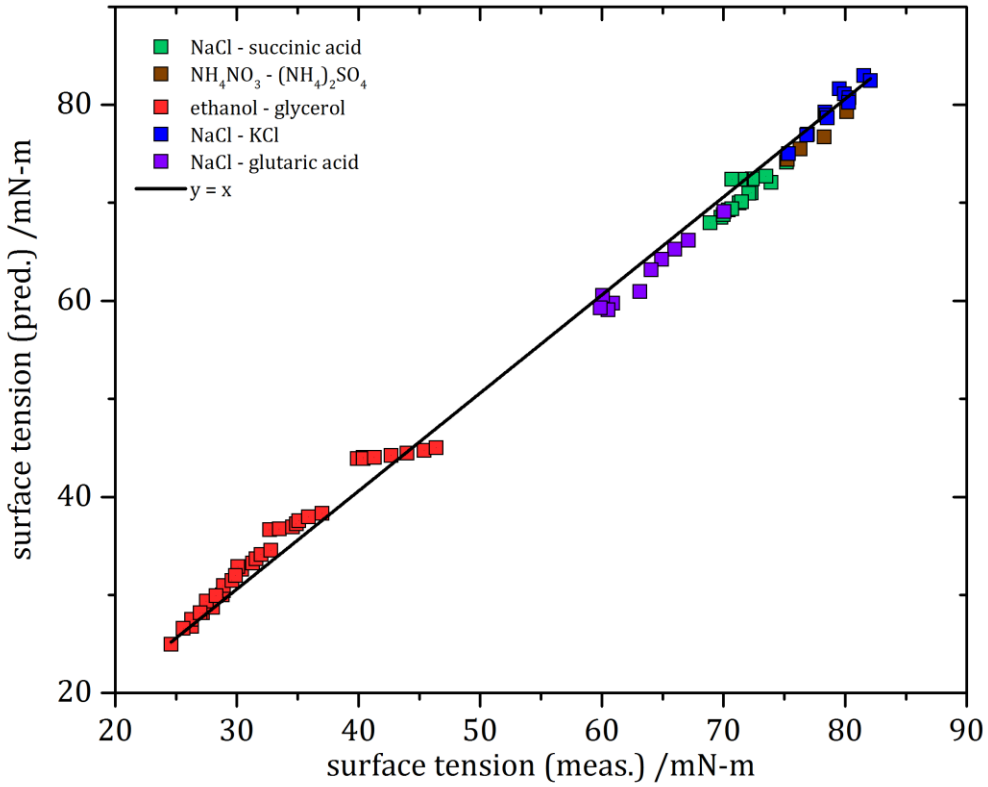

Figure 2: Surface tension model predictions (pred.) vs. surface tension data (meas.) for five ternary systems. For each point, a predicted value was found based on the concentrations of the two solutes in the corresponding measured point. Thus, any variation in the y-axis is purely from change in amount or type of solute. Data sources: NaCl-succinic acid (Vanhanen et al, 2008[42]); NaCl-KCl, (Belton, 1935[43]); NaCl – glutaric acid, optical tweezers; ethanol-glycerol (Ernst et al, 1936[41]); NH_4NO_3 – $(NH_4)_2SO_4$, taken by author with Wilhelmy plate (Digital Tensiometer K10ST by Krüss).

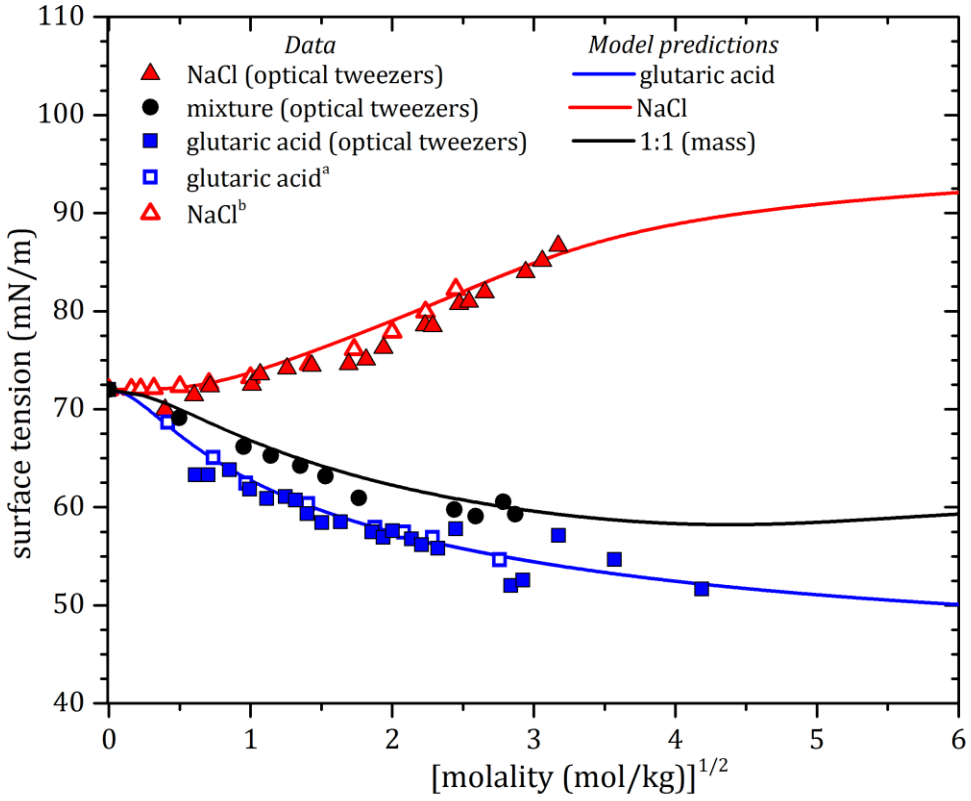

Figure 3: Surface tension model predictions and measurements vs. square root of molality. In the mixture, molality is the sum of the molalities of each solute. Model predictions for the binary systems are found through eq 18. For the mixture, which has a 1:1 composition by mass, there is no fitting to the data presented. Instead, the 6 total model parameters from the binary treatments are applied to eqs 13-17 to produce the curve. Data sources: [a]Boyer and Dutcher, 2016[23]; [b]Washburn et al., 1928.[39]

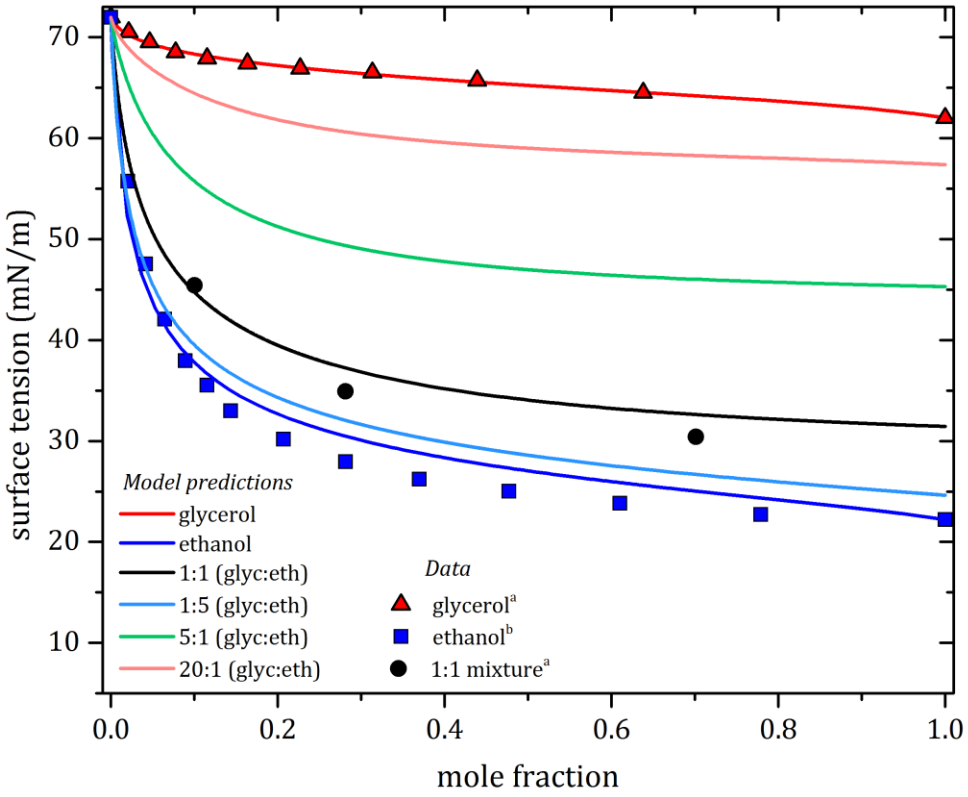

Figure 4: Surface tension (σ) versus mole fraction (x) predictions for ethanol and glycerol aqueous solutions and mixtures (glycerol + ethanol + water) at different glycerol:ethanol (glyc:eth) mole ratios. Also shown are the curves of binary solutions with each solute and a sample of surface tension data for the 1:1 mixture that agree with predictions. Model predictions for the binary systems are found through eq 18. The mole fractions represent the fraction of total amount of solute ($x = x_{glycerol} + x_{ethanol}$). Data sources: [a](Ernst et al, 1936[41]), [b](Vazquez eta l, 1995[38]).

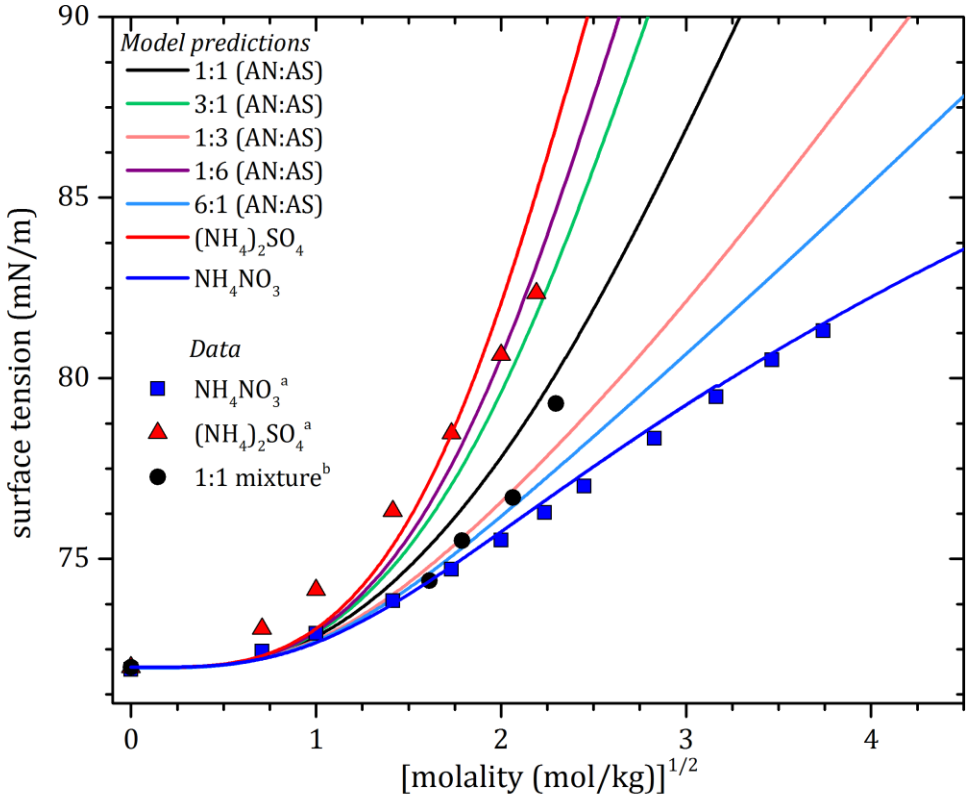

Figure 5: Surface tension model predictions and measurements vs. square root of molality for the ternary system consisting of NH_4NO_3 (AN) and $(NH_4)_2SO_4$ (AS) mixtures in aqueous solutions. Various mole ratios of AN:AS are shown by the curves. In the mixture, molality is the sum of the molalities of each solute. Model predictions for the binary systems are found through eq 18. Data sources: [a]ammonium nitrate and ammonium sulfate (Washburn et al,1928[39]), [b]1:1 mole ratio (measured with Digital Tensiometer K10ST by Krüss).

Supporting Information

A model for an arbitrary number of solutes is derived. Expressions for surface tension, entropy, and parameter *C* are given for 1, 2 and 3 solutes directly from the new model. Residual plots are shown for systems where data are available to compare with model predictions.

Acknowledgments

This material is based upon work supported by the National Science Foundation under Grant No. 1554936. The authors acknowledge funding support for H.C.B. through a National Science Foundation Graduate Research Fellowship. Part of this work was carried out in the College of Science and Engineering Characterization Facility, University of Minnesota, which receives funding from the NSF through the UMN MRSEC under Award DMR-1420013. J.P.R. and B.R.B. acknowledge support from the Engineering and Physical Sciences Research Council (EPSRC) through grant EP/L010569/1. Donald Hall is acknowledged for some of the optical tweezers measurements of supersaturated sodium chloride surface tension.

TOC Graphic

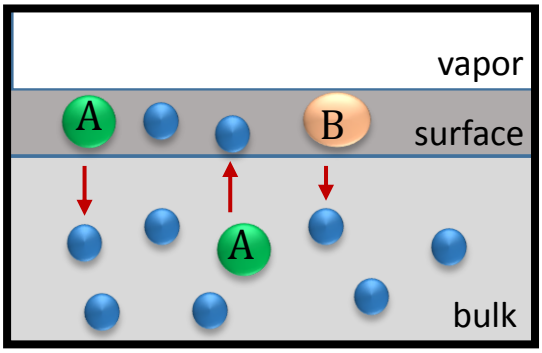

(1) Ruehl, C. R.; Davies, J. F.; Wilson, K. An Interfacial Mechanism for Cloud Droplet Formation on Organic Aerosols. *Science (80-.).* **2016**, *351* (6280), 1447–1450.

(2) Varga, Z.; Kiss, G.; Hansson, H.-C. Modelling the Cloud Condensation Nucleus Activity of Organic Acids. *Atmos. Chem. Phys. Discuss.* **2007**, *7* (2), 5341–5364.

(3) McNeill, V. F; Sareen, Neha; Schwier, A. N. Surface-Active Organics in Atmospheric Aerosols. *Top. Curr. Chem.* **2013**, *339*, 201–259.

(4) Öhrwall, G.; Prisle, N. L.; Ottosson, N.; Werner, J.; Ekholm, V.; Walz, M.-M.; Björneholm, O. Acid–Base Speciation of Carboxylate Ions in the Surface Region of Aqueous Solutions in the Presence of Ammonium and Aminium Ions. *J. Phys. Chem. B* **2015**, *119* (10), 4033–4040.

(5) Venkateshwaran, V.; Vembanur, S.; Garde, S. Water-Mediated Ion-Ion Interactions Are Enhanced at the Water Vapor-Liquid Interface. *Proc. Natl. Acad. Sci. U. S. A.* **2014**, *111* (24), 8729–8734.

(6) Aumann, E.; Hildemann, L. M.; Tabazadeh, a. Measuring and Modeling the Composition and Temperature-Dependence of Surface Tension for Organic Solutions. *Atmos. Environ.* **2010**, *44* (3), 329–337.

(7) Farmer, D. K.; Cappa, C. D.; Kreidenweis, S. M. Atmospheric Processes and Their Controlling Influence on Cloud Condensation Nuclei Activity. *Chem. Rev.* **2015**, *115* (10), 4199–4217.

(8) Faust, J. a.; Dempsey, L. P.; Nathanson, G. M. Surfactant-Promoted Reactions of Cl2 and Br2 with Br- in Glycerol. *J. Phys. Chem. B* **2013**, *117* (41), 12602–12612.

(9) Noziere, B. Dont' Forget the Surface. *Science (80-.).* **2016**, *351* (6280), 1396–1397.

(10) Lee, M.-T.; Brown, M. a.; Kato, S.; Kleibert, A.; Türler, A.; Ammann, M. Competition between Organics and Bromide at the Aqueous Solution–Air Interface as Seen from Ozone Uptake Kinetics and X-Ray Photoelectron Spectroscopy. *J. Phys. Chem. A* **2015**, *119*, 4600–4608.

(11) Yli-juuti, T.; Zardini, A. a; Eriksson, A. C.; Hansen, A. M. K.; Pagels, J. H.; Swietlicki, E.; Svenningsson, B.; Glasius, M.; Worsnop, D. R.; Riipinen, I.; et al. Volatility of Organic Aerosol: Evaporation of Ammonium Sulfate/ Succinic Acid Aqueous Solution Droplets. *Environ. Sci. Technol.* **2013**, *47*, 12123–12130.

(12) Frosch, M.; Prisle, N. L.; Bilde, M.; Varga, Z.; Kiss, G. Joint Effect of Organic Acids and Inorganic Salts on Cloud Droplet Activation. *Atmos. Chem. Phys.* **2011**, *11* (8), 3895–3911.

(13) Li, Z.-B.; Li, Y.-G.; Lu, J.-F. Surface Tension Model for Concentrated Electrolyte Aqueous Solutions by the Pitzer Equation. *Ind. Eng. Chem. Res.* **1999**, *38*, 1133–1139.

(14) Li, Z.; Lu, B. C. On the Prediction of Surface Tension for Multicomponent Mixtures. **2001**, *79*, 402–411.

(15) Hu, Y. F.; Lee, H. Prediction of the Surface Tension of Mixed Electrolyte Solutions Based on the Equation of Patwardhan and Kumar and the Fundamental Butler Equations. *J. Colloid Interface Sci.* **2004**, *269* (2), 442–448.

(16) Lee, J. Y.; Hildemann, L. M. Surface Tension of Solutions Containing Dicarboxylic Acids

with Ammonium Sulfate, D-Glucose, or Humic Acid. *J. Aerosol Sci.* **2013**, *64*, 94–102.

(17) Lee, J. Y.; Hildemann, L. M. Surface Tension of Solutions Containing Dicarboxylic Acids. *Atmos. Environ.* **2014**, *89*, 260–267.

(18) Dutcher, C. S.; Wexler, A. S.; Clegg, S. L. Surface Tensions of Inorganic Multicomponent Aqueous Electrolyte Solutions and Melts. *J. Phys. Chem. A* **2010**, *114* (46), 12216–12230.

(19) Pitzer, K. S. Thermodytriarnics of Electrolytes. I. Theoretical Basis and General Equations. *J. Phys. Chem.* **1973**, *77* (2), 268–277.

(20) Szyszkowski, v. B. Experimentelle Studien Uber Kapillare Eigenschaften Der Wassrigen Losungen von Fettsauren. *Z. Phys. Chem.* **1908**, *64*, 385.

(21) Wexler, A. S.; Dutcher, C. S. Statistical Mechanics of Multilayer Sorption: Surface Tension. *J. Phys. Chem. Lett.* **2013**, *4* (10), 1723–1726.

(22) Boyer, H.; Wexler, A.; Dutcher, C. S. Parameter Interpretation and Reduction for a Unified Statistical Mechanical Surface Tension Model. *J. Phys. Chem. Lett.* **2015**, *6* (17), 3384–3389.

(23) Boyer, H. C.; Dutcher, C. S. Statistical Thermodynamic Model for Surface Tension of Aqueous Organic Acids with Consideration of Partial Dissociation. *J. Phys. Chem. A* **2016**, *120* (25), 4368–4375.

(24) Dutcher, C. S.; Ge, X.; Wexler, A. S.; Clegg, S. L. Statistical Mechanics of Multilayer Sorption: Extension of the Brunauer-Emmett-Teller (BET) and Guggenheim-Anderson-de Boer (GAB) Adsorption Isotherms. *J. Phys. Chem. C* **2011**, *115* (33), 16474–16487.

(25) Dutcher, C. S.; Ge, X.; Wexler, A. S.; Clegg, S. L. Statistical Mechanics of Multilayer Sorption: 2. Systems Containing Multiple Solutes. *J. Phys. Chem. C* **2012**, *116* (2), 1850–1864.

(26) Dutcher, C. S.; Ge, X.; Wexler, A. S.; Clegg, S. L. An Isotherm-Based Thermodynamic Model of Multicomponent Aqueous Solutions, Applicable over the Entire Concentration Range. *J. Phys. Chem. A* **2013**, *117* (15), 3198–3213.

(27) Ohm, P. B.; Asato, C.; Wexler, A. S.; Dutcher, C. S. Isotherm-Based Thermodynamic Model for Electrolyte and Nonelectrolyte Solutions Incorporating Long- and Short-Range Electrostatic Interactions. *J. Phys. Chem. A* **2015**, *119* (13), 3244–3252.

(28) Nandy, L.; Ohm, P. B.; Dutcher, C. S. Isotherm-Based Thermodynamic Models for Solute Activities of Organic Acids with Consideration of Partial Dissociation. *J. Phys. Chem. A* **2016**, *120* (24), 4147–4154.

(29) Bzdek, B. R.; Power, R. M.; Simpson, S. H.; Reid, J. P.; Royall, C. P. Precise, Contactless Measurements of the Surface Tension of Picolitre Aerosol Droplets. *Chem. Sci.* **2016**, *7*, 274–285.

(30) Power, R. M.; Reid, J. P. Probing the Micro-Rheological Properties of Aerosol Particles Using Optical Tweezers. *Rep. Prog. Phys.* **2014**, *77* (7), 074601.

(31) Power, R. M.; Simpson, S. H.; Reid, J. P.; Hudson, a J. The Transition from Liquid to Solid-like Behaviour in Ultrahigh Viscosity Aerosol Particles. *Chem. Sci.* **2013**, *4*, 2597–2604.

(32) Power, R. M.; Burnham, D. R.; Reid, J. P. Toward Optical-Tweezers-Based Force

Microscopy for Airborne Microparticles. *App. Opt.* **2014**, *53* (36), 8522–8534.

(33) Preston, T. C.; Reid, J. P. Accurate and Efficient Determination of the Radius, Refractive Index, and Dispersion of Weakly Absorbing Spherical Particle Using Whispering Gallery Modes. *J. Opt. Soc. Am. B-Optical Phys.* **2013**, *30* (8), 2113–2122.

(34) Bzdek, B. R.; Collard, L.; Sprittles, J. E.; Hudson, A. J.; Reid, J. P. Dynamic Measurements and Simulations of Airborne Picolitre-Droplet Coalescence in Holographic Optical Tweezers. *J. Chem. Phys.* **2016**, *145* (5), 054502.

(35) Rayleigh, L. On the Capillary Phenomena of Jets. *Proc. R. Soc. London* **1879**, *29*.

(36) Lamb, H. *Hydrodynamics*, 6th ed.; Cambridge University Press: Cambridge, 1932.

(37) Cai, C.; Miles, R. E. H.; Cotterell, M. I.; Marsh, A.; Rovelli, G.; Rickards, A. M. J.; Zhang, Y.-H.; Reid, J. P. Comparison of Methods for Predicting the Composition Dependence of the Density and Refractive Index of Organic-Aqueous Aerosols. *J. Phys. Chem. A* **2016**, *120*, 6604–6617.

(38) Vasquez, G.; Alvarez, E.; Navaza, J. M. Tension of Alcohol + Water from 20 to 50 °C. *J. Chem. Eng. Data* **1995**, *40* (3), 611–614.

(39) Washburn, E.; West, C. J.; Hull, C. *International Critical Tables of Numerical Data, Physics, Chemistry, and Technology*; 1928; Vol. 4.

(40) Hyvärinen, A.; Lihavainen, H.; Gaman, A.; Vairila, L.; Ojala, H.; Kulmala, M.; Palme, E. Surface Tensions and Densities of Oxalic, Malonic, Succinic, Maleic, Malic, and Cis - Pinonic Acids. *J. Chem. Eng. Data* **2006**, *51*, 255–260.

(41) Ernst, R. C.; Watkins, C. H.; Ruwe, H. H. The Physical Properties of the Ternary System Ethyl Alcohol-Glycerin-Water. *J. Phys. Chem.* **1936**, *40* (5), 627.

(42) Vanhanen, J.; Hyvärinen, A.-P.; Anttila, T.; Raatikainen, T.; Viisanen, Y.; Lihavainen, H. Ternary Solution of Sodium Chloride, Succinic Acid and Water; Surface Tension and Its Influence on Cloud Droplet Activation. *Atmos. Chem. Phys.* **2008**, *8*, 4595–4604.

(43) Belton, J. W. The Surface Tensions of Ternary Solutions. Part III. *Trans. Faraday Soc.* **1935**, *31*, 1648–1652.